Chapter 2
Impedance Spectroscopy and Experimental Setup

2.1 Introduction

The objective of this chapter is to introduce the measuring instruments and software programs used for the experimental setup. It provides the reader a detailed insight of, electrochemical impedance spectroscopy basics and data representation along with highlighting the methodology of measurement data collection. It explains all the hardware and software used to collect the impedance data and the models involved in analyzing the acquired information. It also describes the interfacing of the measuring instruments with LabVIEW program to obtain a standalone automated measurement system. It provides an account of the significant applications of impedance spectroscopy method for characterization of sensors and material under test (MUT). The objectives are to measure and characterize the developed sensors according to EIS models and methods. Mathematical methods like complex non-linear least square curve fitting were used to deduce equivalent circuit to the electrochemical cell under test. The parameters obtained from the measuring instruments are frequency, *f*, impedance, Z and phase angle. Mathematical methods used to interpret these into real and imaginary parts in the complex plane for analysis of impedance characteristics are also discussed.

2.2 Electrochemical Impedance Spectroscopy

Electrochemical Impedance Spectroscopy (EIS) has seen a huge boost in popularity in recent time due to its extraordinary sensitivity. It is used to evaluate electrical properties of materials and their interfaces with surface-modified electrodes [1]. This method has been widely used to study of electrochemistry [2, 3], biomedical applications [4, 5], material science [6] and others. J. Ross Mcdonald in [7] describes the EIS as a part of Impedance measurement using AC polarography involving electrochemical reactions. The response of an electrochemical cell to a low amplitude sinusoidal perturbation as a function of frequency and has been

A.I. Zia and S.C. Mukhopadhyay, *Electrochemical Sensing: Carcinogens in Beverages*, Smart Sensors, Measurement and Instrumentation 20,
DOI 10.1007/978-3-319-32655-9_2

reported to estimate the dielectric properties of milk [8], meat inspection [9], quality testing in leather [10], Saxophone reed inspection [11], detection of contaminated seafood with marine biotoxin [12], food endo-toxins [12–16], evaluate electrical properties of drinks, and water [17]. EIS involves measurements and analysis of materials involving ionic conduction in solid and liquid electrolytes. Ionically conducting glasses and polymers, fused salts, and nonstoichiometric ionically bonded single crystals have been used for impedance measurements where conduction can involve motion of ion vacancies and interstitials. EIS is also conducted to study of fuel cells, rechargeable batteries, and corrosion. Another category of IS applies to dielectric materials: solid or liquid non-conductors whose electrical characteristics involve dipolar rotation, and to materials with predominantly electronic conduction [18]. System Impedance may be measured using various techniques. The most cited impedance measurement techniques are given as follows.

2.2.1 AC Bridges

This is the oldest of all the techniques initially used for the measurement of double-layer parameters, principally of the hanging mercury drop electrode. It has also been used to measure the electrode impedance in a faradaic reaction to evaluate the dynamic processes at the electrode. Although this method is slow, yet provides a magnificent precision of measurements.

2.2.2 Lissajous Curves

Formation of elliptical figures as a result of the simultaneous application of the applied AC voltage and resulting AC current to a twin beam oscilloscope is called Lissajous curves. Analyzes of Lissajous curves produced on twin channel oscilloscope screens was used to perform impedance measurements and had been an accepted method for impedance spectroscopy prior to the advent of modern EIS instrumentation. The measurement time involved in using this technique (often up to many hours) is long enough for a chemical cell to cause drift in its system parameters. The cell can change through adsorption of impurities, oxidations, degradations, temperature variations, etc. These curves have been used to determine the impedance, but frequency limitations and sensitivity to noise has limited the use of this technique. Figure 2.1 shows the formation of Lissajous figures as a consequence of two out of phase signals.

2.2.3 Fast Fourier Transforms (FFT)

The Fast Fourier Transforms is a mathematical method to evaluate the system impedance. Taking the Fourier transform of the perturbation signal in time domain

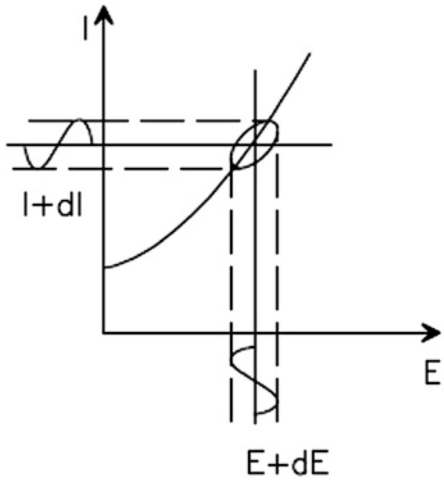

Fig. 2.1 Formation of Lissajous figure

and generation of corresponding frequency domain data using a computerized algorithm is referred as FFT. FFT provides a fast and efficient algorithm for computation of the Fourier transforms. In practice, only limited length data is transformed, causing the broadening of the computer frequency spectrum, commonly called 'leakage'. Another problem called 'aliasing' is linked with the presence of the frequencies larger than one-half of the time domain sampling frequency.

2.2.4 Phase Sensitive Detections (PSD)

Phase sensitive detection is used in lock-in amplifiers interfaced with precision potentiostats for system impedance measurements. It contains one time-independent component, depending on the phase difference between two signals and proportional to the amplitude of the measured AC signal. The output signal is applied to a low-pass filter that averages the signal component having frequencies above the cut-off frequency. The disadvantage of the lock-in technique is that it retains the combination of harmonic frequencies present in the input signal.

2.2.5 Frequency Response Analysis (FRA)

Frequency Response Analyzers are hi precision instruments that determine the frequency response of the standardized system. The operation of FRA is based on interpreting correlation of the studied signal with the reference perturbation. The measured signal is multiplied by the sine and cosine of the reference signal of the same frequency and integrated over one time period. Real and imaginary parts of the measured signal are recovered, strictly rejecting all harmonics. The advantage of the correlation process is a reduction of noise, but it is achieved at the cost of attenuation of the output signal.

Among a number of methods available for impedance measurements, FRA has become a de facto standard for EIS. FRA is a single sine-wave input method in which a small amplitude (5–15 mV) AC sine wave of a given frequency is overlaid on a dc bias potential, applied to the working/excitation electrode and measurement of resulting AC current is made. The system remains pseudo-linear at low-amplitude AC potential. The process is repeated for the desired frequency range, and impedance is computed for five to ten measurements per decade change in frequency. In order to ensure the system linearity, stability, and repeatability, this method is rendered viable only for a stable and reversible system in equilibrium. For this reason, instantaneous impedance measurements are mandatory for non-stationary systems [19]. A non-linear system will contain harmonics (noise) in the measured current response. The drift in the measured system parameters is often observed if the system loses its steady state during the measurement time. The electrochemical cell can change through adsorption, oxidation, coating degradation and temperature variations; to list, these are a few major factors affecting the steady-state condition of the system under test. EIS is used to deduce the changes taking place in the electrochemical system in general and observe the changes in the conductance and capacitance at the sensing surface, interface, and layers, in particular. Next section discusses the fundamental concepts of impedance spectroscopy.

2.2.6 Electrochemical Impedance Spectroscopy; Theory and Analyses

In practice, electrochemical cells are an example of complex non-linear systems. The relationship between current and voltage is highly non-linear. Pseudo-linearity of the electrochemical system is achieved by considering a small linear part of the I-V curve as shown in Fig. 2.2.

Pseudo-linearity is quite useful because; cell's substantial non-linear response to Direct Current (DC) potential is not observable as current is measured at excitation frequency; the measured current is independent of harmonics. If the system is non-linear, the current response of the system will be deformed by the harmonics. The system under test must remain in steady-state throughout the testing time; this is another stringent condition that may affect system linearity. With the advent of hi precision fast FRAs and computing systems, this problem could be catered for. For example, it takes only 88 ms for Hioki 3522-50 to measure impedance, at a particular frequency, without compromising the accuracy of 99.95 % while operating at slow mode; refer to Hioki 3522-50 specification sheet shown in Table 2.1.

In a pseudo-linear electrochemical cell, the impedance can be measured by applying a low-amplitude AC perturbation, E_t, and measuring the phase shift appearing in consequent alternating current flowing through the sensor with

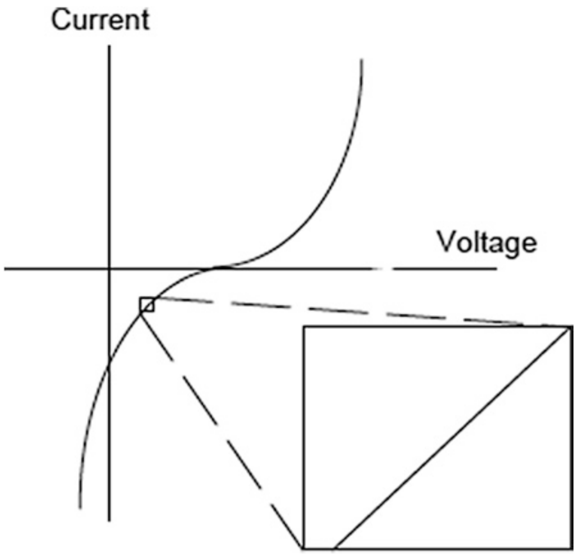

Fig. 2.2 I-V curve for a non-linear system. Pseudo-linearity of the system is achieved by considering a small part of the curve

reference to the applied signal. The magnitude of the occurring phase shift depends on the impedance offered to the electron flow by nature of the electrolyte, diffusion, electrode kinetics and chemical reactions happening inside the cell. Figure 2.3 shows a phase shift ө in the received, current signal with reference to the applied potential perturbation.

Impedance (Z) is a measure of the circuit characteristics to impede the flow of electrons through the circuit, measured in Ohm when exposed to periodic electrical perturbations. The reciprocal of impedance is called admittance, denoted by Y and measured in Siemens (S). Mathematically, impedance is expressed as a complex number comprising of resistance and reactance. Resistance is a static property of the system and is independent of the incident Alternating Current (AC) frequency. It is represented by the real part of the compound number, denoted as R_e, Z_{real}, *or* Z'. On the other hand, reactance is purely frequency dependent and appears in capacitors and inductors consequent to the applied AC frequency. Reactance is represented by the imaginary part of the complex impedance and is symbolized by R_{im}, X_c or Z_c'' for capacitive reactance and X_L or Z_L'' for inductive reactance, respectively. The basic Ohm's law in Eq. 2.1 defines the resistance R in term potential, V, and current I as;

$$R = \frac{V}{I} \tag{2.1}$$

whereas, Ohm's law for alternating current defines impedance Z in terms of time-dependent alternating potential E_t, and current I_t as:

$$Z = \frac{E_t}{I_t} \tag{2.2}$$

Table 2.1 Hioki Hi Precision LCR 3522-50 and 3532-50 Specifications

Specifications		
	3522-50	3532-50
Measurement parameters	|Z|, |Y|, θ, Rp (DCR), Rs (ESR, DCR). G, X, B, Cp, Cs, Lp, Ls, D, Q	|Z|, |Y|, θ, Rp, Rs (ESR), G, X, B, Cp, Cs, Lp, Ls, D, Q
Measurement ranges: |Z|, R, X	10.00 mΩ–200.00 MΩ (depending on measurement frequency and signal levels)	
θ	−180.00° to +180.00°	
C	0.3200 pF–1.0000 F	0.3200 pF–370.00 mF
L	16.000 nH–750.00 kH	
D	0.00001–9.99999	
Q	0.01–999.99	
|Y|, G, B	5.0000 nS–99.999 S	
Basic accuracy	Z: ± 0.08 % rdg. θ ± 0.05°	
Measurement frequency	DC, 1 MHz–100 kHz	42 Hz–5 MHz
Measurement signal levels	10 mV–5 V rms/10μA–00 mA rms	
Output impedance	50 Ω	
Display screen	LCD with backlight/99,999 (full 5 digits)	
Measurement time (Typical values for displaying |Z|)	Fast: 5 ms	Fast: 5 ms
	Normal: 16 ms	Normal: 21 ms
	Slow 1: 88 ms	Slow 1: 72 ms
	Slow 2: 828 ms	Slow 2: 140 ms
Settings in memory	Max. 30 Sets	
Comparator functions	HI/IN/LO settings for two measurement parameters; percentage, Δ%, or absolute value settings	
DC Bias	External DC bias ± 40 V max. (option)	
External printer	9442 printer (option)	
External interfaces	GP-IB or RS-232C (Options), external I/O for sequencer use	
Power source	100, 120, 220 or 240 V(± 10 %) AC (selectable), 50/60 Hz	
Maximum rated power	40 VA approx	50 VA approx

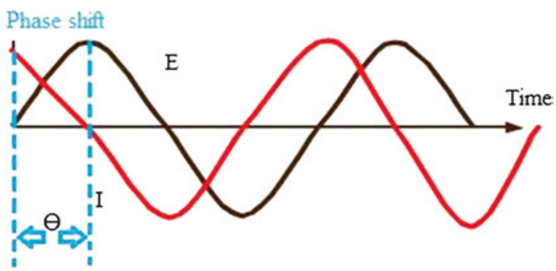

Fig. 2.3 Phase shift in current I_t as a response to excitation-potential E_t in a linear system

The excitation signal can be expressed as a function of time;

$$E_t = E_0 \sin \omega t \tag{2.3}$$

where E_t is the potential difference at time t, E_0 is the amplitude of the voltage signal at $t = 0$, and ω is the angular frequency given by ($\omega = 2\pi f$) expressed in radians/second and frequency, *f,* in hertz.

For a linear system, the response signal I_t, has a phase shift,θ, with amplitude of I_0 which can be expressed by:

$$I_t = I_0 \sin(\omega t - \theta) \tag{2.4}$$

An expression in Eq. 2.2 for Ohm's Law can be used to calculate the impedance of the system given by;

$$Z = \frac{E_t}{I_t} = \frac{E_0 \sin \omega t}{I_0 \sin(\omega t - \theta)}$$
$$Z = Z_0 \frac{\sin(\omega t)}{\sin(\omega t - \theta)} \tag{2.5}$$

The impedance, Z, now can be expressed in term of a magnitude of Z_0 and a phase shift, θ. Equation 2.5 can also be expressed in term of Euler's relationship given by;

$$e^{j\theta} = \cos \theta + jsin\theta \tag{2.6}$$

where $j = \sqrt{-1}$ ('j' is preferred by electrochemists instead of 'i')

The impedance, Z, can be expressed in term of potential, E, and current response, I, given by;

$$E_t = E_0 e^{j\omega t} \tag{2.7}$$

$$I_t = I_0 e^{j(\omega t -)\theta} \tag{2.8}$$

Therefore the impedance, Z;

$$Z(\omega) = \frac{E_t}{I_t} = \frac{E_0 e^{j\omega t}}{I_0 e^{j(\omega t - \theta)}} = Z_0 e^{j\theta} \tag{2.9}$$

$$Z(\omega) = Z_0(\cos\theta + j\sin\theta) \tag{2.10}$$

The impedance now is in the form of real part (Z_0 cosθ) and imaginary part (Z_0 sinθ) represented as follows:

$$\mathrm{Re}Z = Z' = Zreal = Z_0 \cos \theta \tag{2.11}$$

$$Z'' = Zimag = Z_0 \sin \theta \tag{2.12}$$

The raw data for all measured frequencies in EIS experiments comprises of the real and imaginary components of potential difference E′ and E″ and the real and imaginary components of current I′ and I″ respectively. The phase shift (ɵ) and total impedance (Z) are the two basic parameters calculated out of the raw data using equations given in Table 2.3. For data analysis purpose, the calculated impedance characteristics are expressed as Nyquist plot and Bode plot.

2.2.7 'Nyquist' and 'Bode' Plots for Impedance Data Analysis

Nyquist plot also known as Cole-Cole plot is one of the most critical and popular formats for evaluating electrochemical parameters like electrolytic solution resistance (R_s), electrode polarization resistance (R_p) and double layer capacitance (C_{dl}), etc. These parameters shall be discussed in detail in the following sections. Nyquist plot represents $Z'(\omega)$ and $Z''(\omega)$ in a complex plane. Among several advantages of Nyquist plot; calculation of solution resistance by extrapolating the curve to x-axis; observable effects of solution resistance; emphasis on the series circuit; comparison of the results of two or more separate experiment, are a few major advantages. One major disadvantage of Nyquist plot is that information on frequency is lost which makes the calculation of C_{dl} complicated.

Bode plot represents absolute $Z(\omega)$ and phase angle $\theta(\omega)$ in the frequency domain. Since frequency appears at one of the axes, the effect of the spectrum on the impedance and phase drift is obvious. R_s, R_p, C_{dl} and frequency values, where phase shift $\theta(\omega)$ is maximum/minimum, can be evaluated using Bode plot. This format is desirable when data-scatter prevents adequate fitting of the Nyquist plot. Due to these edges, researchers declare Bode plot as a clearer description of electrochemical cell's frequency-dependant behavior compared to Nyquist plot.

A flow diagram developed by McDonald [18], shown in Fig. 2.4, has been followed by analysis of the electrochemical research on detection of hormones and EDCs presented in this thesis. In order to understand the significance and methods to extract electrochemical cell's parameters, Randle's electrochemical cell model was used to deduce equivalent circuit for the electrochemical cell under test. Complex Nonlinear Least Square (CNLS) curve fitting technique was applied to extract equivalent circuit and component parameters.

2.2.8 Randle's Electrochemical Cell Equivalent Circuit Model

This model was introduced by Randle in 'Discussion of the Faraday Society' in 1947 [20]. The model provides the account of mixed kinetic processes taking

Fig. 2.4 Flow chart for the measurement and characterization of a material-electrode system by EIS [18]

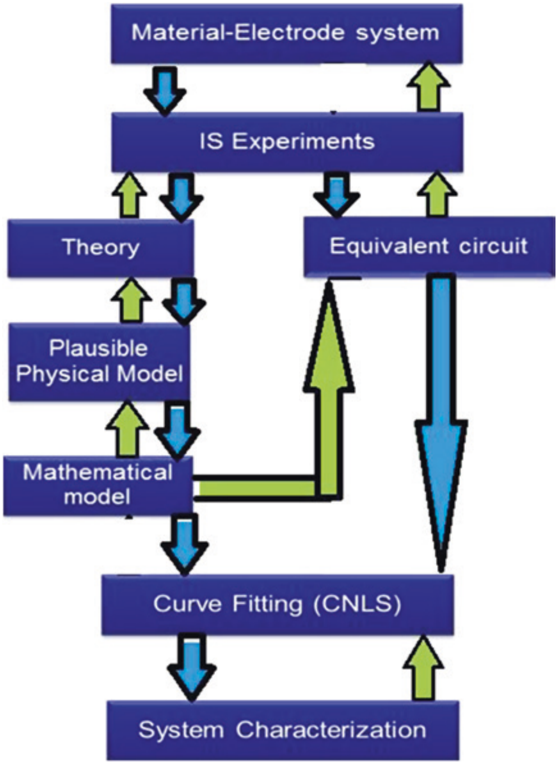

place at the electrode-electrolyte interface. These processes include the fast mass transfer reaction, slow-paced charge transfer reaction, and diffusion processes at the interface. A double layer capacitance is observed at the interface due to the presence of Outer Helmholtz Plane (OHP) and Inner Helmholtz Plane (IHP) at the electrode surface as shown in Fig. 2.5.

The Randle's cell includes double-layer capacitance, C_{dl}, solution resistance, R_s, charge/electron transfer resistance, R_{ct} and Z_W as shown Fig. 2.6 in the electrochemical cell equivalent circuit deduced in [20].

The expression for the absolute impedance as a function of frequency is given as;

$$Z(\omega) = R_s + \frac{R_{ct}}{1 + \omega^2 R_{ct}^2 C_{dl}^2} - \frac{j\omega R_{ct}^2 C_{dl}}{1 + \omega^2 R_{ct}^2 C_{dl}^2} \tag{2.13}$$

where the real part (Z') is given by;

$$Z'(\omega) = R_s + \frac{R_{ct}}{1 + \omega^2 R_{ct}^2 C_{dl}^2} \tag{2.14}$$

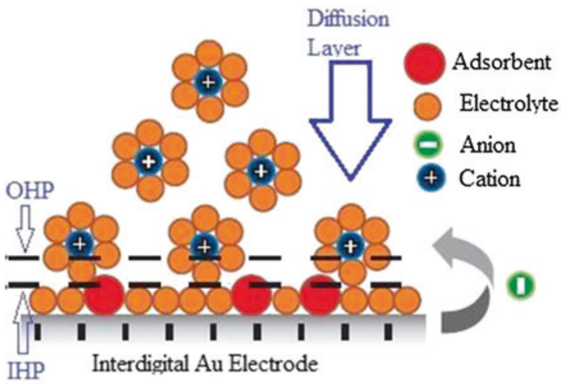

Fig. 2.5 Kinetic processes taking place at electrode-electrolyte interface (Randle's cell model)

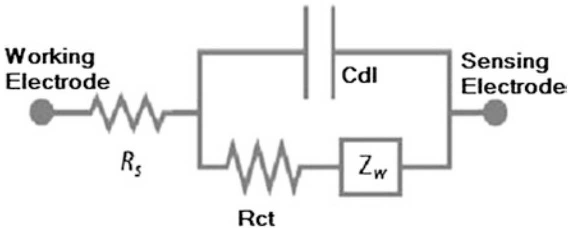

Fig. 2.6 Randle's electrochemical cell equivalent circuit model

and the imaginary part (Z″) is given by;

$$Z''(\omega) = -\frac{\omega R_{ct}^2 C_{dl}}{1 + \omega^2 R_{ct}^2 C_{dl}^2} \tag{2.15}$$

The impedance spectra from the experimental results depicted electrode and electrolyte are related by a mixed kinetic and diffusion processes at the electrode surface which causes a polarization at the interface. R_{ct} is, therefore, sometimes referred as polarization resistance, denoted as $R_{p,}$ in EIS literature. The value of 'charge transfer resistance $R_{ct,}$ r polarization resistance R_p′ can be calculated from Bode or Nyquist plot. The rate of an electrochemical reaction can be strongly influenced by diffusion of reactants towards, or away from the electrode-electrolyte interface. This situation can exist when the electrode is covered with adsorbed solution components or a selective coating. An addition element called Warburg impedance, $Z_{W,}$ appears in series with resistance R_{ct}. Mathematically Warburg impedance is given by;

$$Z_W = \frac{\sigma_w}{\sqrt{j\omega}} \tag{2.16}$$

where, σ_W is called Warburg diffusion coefficient. It appears that the characteristic of the Warburg impedance is a straight line with a slope of 45° at a lower frequency. This refers to low-frequency diffusion control because the diffusion of reactants to the electrode surface is a slow-paced process which can happen at low frequencies only. At higher frequencies, however, the reactants do not have enough time to diffuse. The slope of this line gives Warburg diffusion coefficient. The Nyquist plot in Fig. 2.7 shows the diagonal line of diffusion process (Warburg impedance) at low frequency. The charge transfer process at higher frequency is illustrated by a single time constant semi-circle curve.

The Nyquist plot for a Randle's cell is always a semicircle due to an RC parallel equivalent circuit. The solution resistance R_s also referred as 'uncompensated solution resistance' denoted as 'R_Ω' in EIS literature can be calculated by high-frequency intercept on the real axis. High-frequency intercept lies closer to the origin of the plot. In Fig. 2.7 it could be read as 25 kΩ. The real axis value at the other (low frequency) intercept is the sum of solution and polarization resistance. The low-frequency intercept could be read by interpolating the semi-circle to the real axis. (In Fig. 2.7 it reads as 325 kΩ). The diameter of the semicircle is, therefore, equal to the polarization resistance (300 kΩ in this case). Figure 2.8 shows the absolute impedance, Z, versus frequency and phase angle in degree with respect to the applied frequency, *f* in Hz. The two plots combined together are referred as Bode plot. Figure 2.9 shows a combined Bode plot for an electrochemical system with Z (absolute) plotted on the primary y-axis and phase (degree) plotted along the secondary y-axis. Frequency is plotted on the x-axis. This format of Bode plot is a useful alternative to calculating solution resistance (R_s or R_Ω), polarization resistance (R_p or R_{ct}) and C_{dl}. Furthermore, $\log(Z_{abs})$ versus $\log(\omega)$ plot sometimes allow a more efficient extrapolation of the data from higher frequencies.

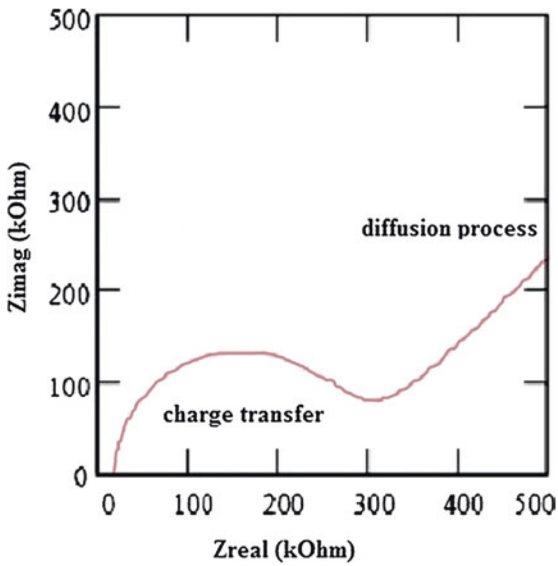

Fig. 2.7 Nyquist plot for Randle's electrochemical cell model [19]

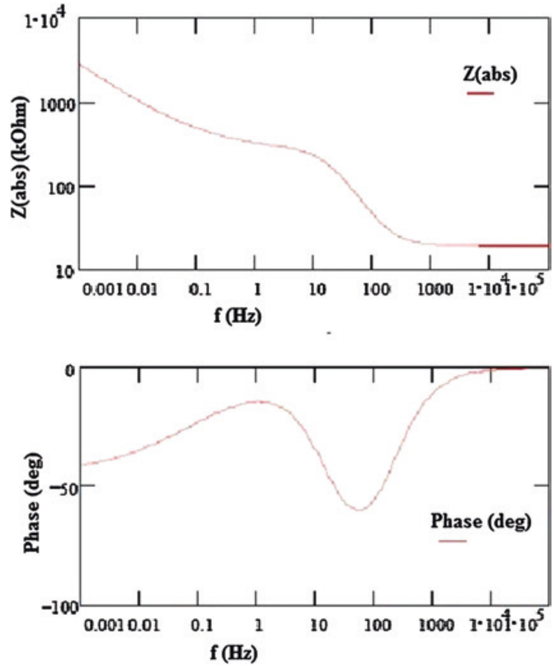

Fig. 2.8 Bode plot for Randle's electrochemical cell model [19]

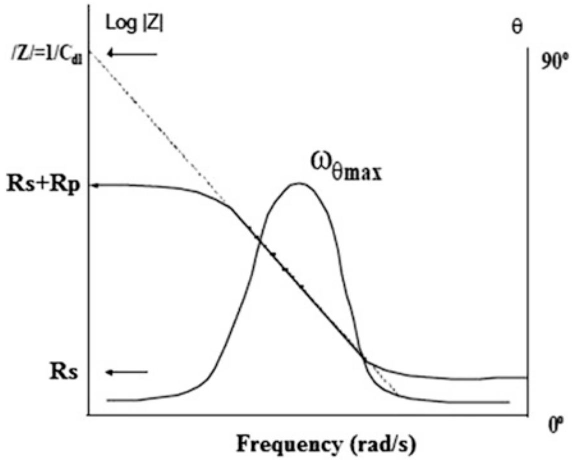

Fig. 2.9 Extraction of intrinsic parameters from bode plot [19]

2.3 Experimental Setup

The experiment setup mainly consisted of Hi-precision Hioki 3522-50 LCR meter, Hioki 4-terminal probe 9140, digital thermometer and humidity tester interfaced through RS232 to a tailor-made LabVIEW program executing on a desktop data

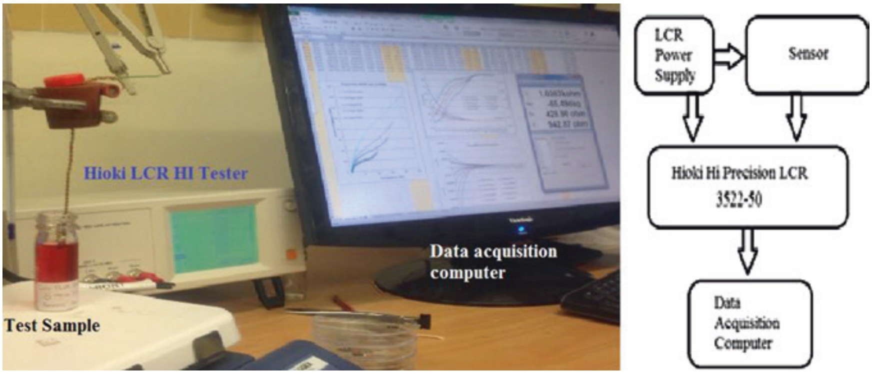

Fig. 2.10 Laboratory test bench with Hioki Hi Precision LCR and data acquisition system

acquisition computer. The temperature, humidity, and inert atmosphere controls were achieved by placing the sensor inside a desiccator, whenever required, to perform the testing under stringent environmental conditions. MicroSuite Laboratory, a research facility available to the School of Engineering and Advanced Technology, Massey University, Palmerston North was used to conduct all set of experiments. Figure 2.10 shows the main experimental setup and the block diagram of the laboratory setup and apparatus used for this research in addition to other in-lab available facilities for heating, cooling, auto enclave, chromatography, microscopy, and spectrophotometry, etc.

2.3.1 Equipment and Instrumentations

The high precision LCR meter Hioki 3522-50 and 3532-50 have been used to obtain test parameters' measurements in order to perform investigation electrochemical impedance spectroscopy from 1 to 5 MHz range as required. The technical specifications of the high-performance set of test equipment LCR meter Hioki 3522-50 and 3532-50 are given in Table 2.1. Figure 2.11 shows the front panel of Hioki high precision LCR meter 3522-50.

2.3.2 Fixture and Test Probe Connections

The standard fixture is a four-wire type Hioki 9261 which can be used for all test frequencies from DC to 5 MHz. Figure 3.3 shows Hioki 9140 4-terminal test probe with crocodile clip termination which can be used for testing in a range of 1 MHz–100 kHz. There are two sets of terminals connecting the sensor to the test

Fig. 2.11 Hioki (Japan) 3522-50 LCR Hi-tester

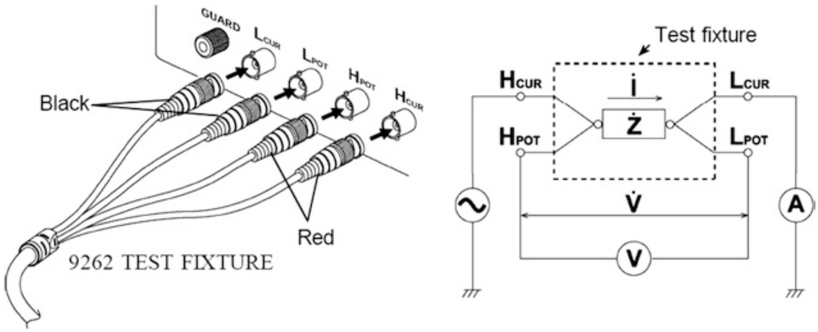

Fig. 2.12 Connecting LCR3522-50/3532-50 to the 9262 test fixture and developed interdigital sensing system

equipment. The outer set of terminals, named H_{CUR} and L_{CUR} on the front panel, are used to measure the current flowing through the sensor, whereas, the inner set of terminals, appointed as H_{POT} and $L_{POT,}$ measure the potential across the sensor at any instant of time. Detail description is shown in Fig. 2.12. Table 2.2 displays the details of fixture connection with shielding to the device under test (DUT).

2.3.3 RS-232C Interface for 3522-50/3532-50 LCR Hi Tester

An RS-232C was used to interface Hioki LCR3522-50 to a desktop/laptop computer in order to develop an automatic data acquisition system. Use of the interface made it possible to control all the functions of the LCR3522-50/3532-50 using software algorithm. The graphical user interface was developed in Labview software to input setting parameters except power on/off. The program consisted of commands and queries made by the data acquisition computer system to the interfaced instrument. A command sent is a set of instructions or data to setup the test conditions

Table 2.2 Hioki Hi Precision LCR test terminals description

Test Terminal	Description
H_{CUR}	Carries the signal current source. Connected to the excitation electrodes of the interdigital sensor
H_{POT}	Detected high voltage sense terminal. Measure potential difference at any instant of time
L_{POT}	Detected low voltage sense terminal
L_{CUR}	Test Current detection terminal
GUARD	Connected to the GND input to minimize noise

Table 2.3 LCR testing parameters and calculation equations

Parameter	Series equivalent circuit mode	Parallel equivalent circuit mode
Z	$\lvert Z\rvert = V/I(= \sqrt{R^2 + X^2})$	
Y	$\lvert Y\rvert = 1/\lvert Z\rvert(=\sqrt{G^2 + B^2})$	
R	$Rs = ESR = \lvert\lvert Z\rvert\cos\theta\rvert$	$Rp = \lvert 1/\lvert Y\rvert\cos\emptyset\rvert(=1/G)$
X	$X = \lvert\lvert Z\rvert\sin\theta\rvert$	
G		$G = \lvert\lvert Y\rvert\cos\emptyset\rvert$
B		$B = \lvert\lvert Y\rvert\sin\emptyset\rvert$
L	$Ls = X/\omega$	$Lp = 1/\omega B$
C	$Cs = 1/\omega X$	$Cp = B/\omega$
D	$D = \lvert 1/\tan\theta\rvert\,\lvert$	
Q	$Q = \lvert\tan\theta\rvert = (1/D)$	

communicated to the LCR meter, whereas query is a set of data or status information requested from the LCR meter. The LCR transmitted the measured/calculated parameters in response to the queries made by the data acquisition computer. The software echoed back the received automatic measurements of the required parameters' data on the computer monitor via a graphical user interface in addition to writing/saving it in Microsoft Excel worksheet in 'xls' format. Table 2.3 provides the details of the parameters measured and calculated by LCR3522-50/3532-50 using the mathematical equations mentioned against each parameter. The data acquisition computer system was used to analyse further the saved information to study the impedance characteristics of the developed sensors and material under test.

2.3.4 Conclusions

The experimental setup, instrumentation, program and measurement methods have been discussed in this chapter. High precision LCR meter's interface with the LABVIEW program has been established in order to erect a stand-alone automatic measurement system. Details of the experimental setup, connection cables, instruments settings, and program interface were explained in the chapter. The basic theory of measurement method using Impedance Spectroscopy (IS) has also been discussed to enlighten the reader with the basic measurement methodology. The setup has been built to a stage where it could be interfaced with a smart sensing transducer that could fetch the information from the electrochemical cell, interpret it into required electrical signal so that valuable information about the kinetic processes taking place inside the cell could be extracted. Development of a sensitive, selective and reliable sensor was the most important part of this research project. The details of the development of the smart sensor are discussed in the following chapter.

References

1. E.J. Olson, P. Buhlmann, Minimizing hazardous waste in the undergraduate analytical laboratory: a microcell for electrochemistry. J. Chem. Educ. **87**(11), 1260–1261 (2010)
2. M. Khafaji, S. Shahrokhian, M. Ghalkhani, Electrochemistry of levo-thyroxin on edge-plane pyrolytic graphite electrode: application to sensitive analytical determinations. Electroanalysis **23**(8), 1875–1880 (2011)
3. J. Fischer, H. Dejmkova, J. Barek, Electrochemistry of pesticides and its analytical applications. Curr. Org. Chem. **15**(17), 2923–2935 (2011)
4. C. Valero Vidal, A. Igual Muñoz, Effect of physico-chemical properties of simulated body fluids on the electrochemical behaviour of CoCrMo alloy". Electrochim. Acta **56**(24), 8239–8248 (2011)
5. C. Wolner, G.E. Nauer, J. Trummer et al., Possible reasons for the unexpected bad biocompatibility of metal-on-metal hip implants. Mater. Sci. Eng., C **26**(1), 34–40 (2006)
6. C. Xhoffer, K. Van den Bergh, H. Dillen, Electrochemistry: a powerful analytical tool in steel research. Electrochim. Acta **49**(17), 2825–2831 (2004)
7. J.R. Macdonald, Impedance spectroscopy. Ann. Biomed. Eng. **20**(3), 289–305 (1992)
8. S.C. Mukhopadhyay, C.P. Gooneratne, G.S. Gupta et al., A low-cost sensing system for quality monitoring of dairy products. Instrum. Measur. IEEE Transac. **55**(4), 1331–1338 (2006)
9. S.C. Mukhopadhyay, C.P. Gooneratne, A novel planar-type biosensor for noninvasive meat inspection. Sens. J. IEEE **7**(9), 1340–1346 (2007)
10. S. Mukhopadhyay, S.D. Choudhury, T. Allsop et al., Assessment of pelt quality in leather making using a novel non-invasive sensing approach. J. Biochem. Biophys. Methods **70**(6), 809–815 (2008)
11. S.C. Mukhopadhyay, G.S. Gupta, J.D. Woolley et al., Saxophone reed inspection employing planar electromagnetic sensors. Instrum. Meas. IEEE Transac. **56**(6), 2492–2503 (2007)
12. M. Rahman, S.B. Abdul, S.C. Mukhopadhyay et al., Novel sensors for food inspections, Sens. Trans. (1726–5479) **114**(3) 2010
13. A. Mohd Syaifudin, S. Mukhopadhyay, P. Yu et al., Characterizations and performance evaluations of thin film interdigital sensors for Gram-negative bacteria detection. pp. 181–186
14. A. Mohd Syaifudin, S. Mukhopadhyay, P. Yu et al., Detection of natural bio-toxins using an improved design interdigital sensors. pp. 1028–1031
15. A. Mohd Syaifudin, S. Mukhopadhyay, P. Yu, Modelling and fabrication of optimum structure of novel interdigital sensors for food inspection, Int. J. Numer. Model. Electron. Netw. Devices Fields **25**(1), pp. 64–81 (2012)
16. M.S. Abdul Rahman, S.C. Mukhopadhyay, P.-L. Yu et al., Detection of bacterial endotoxin in food: new planar interdigital sensors based approach, J. Food Eng. **114**(3), pp. 346–360 (2013)

17. A.I. Zia, A.R. Mohd Syaifudin, S.C. Mukhopadhyay et al., MEMS based impedimetric sensing of phthalates. pp. 855–860
18. E. Barsoukov, J.R. Macdonald, Impedance spectroscopy: theory, experiment, and applications: Wiley-Interscience (2005)
19. B.-Y. Chang, S.-M. Park, Electrochemical impedance spectroscopy. Ann. Rev. Anal. Chem. **3**, 207–229 (2010)
20. J.E.B. Randles, Kinetics of rapid electrode reactions. Discuss. Faraday Soc. **1**, 11–19 (1947)

http://www.springer.com/978-3-319-32654-2

Electrochemical Sensing: Carcinogens in Beverages
Zia, A.I.; Mukhopadhyay, S.C.
2016, XII, 148 p. 121 illus., 6 illus. in color., Hardcover
ISBN: 978-3-319-32654-2